

Zeitschrift: Schweizerische mineralogische und petrographische Mitteilungen =
Bulletin suisse de minéralogie et pétrographie

Band: 80 (2000)

Heft: 3

Artikel: Epitaxy of hedenbergite whiskers on babingtonite in Alpine fissures at
Arvigo, Val Calanca, Grisons, Switzerland

Autor: Armbruster, Thomas / Stalder, Hans Anton / Gnos, Edwin

DOI: <https://doi.org/10.5169/seals-60967>

Nutzungsbedingungen

Die ETH-Bibliothek ist die Anbieterin der digitalisierten Zeitschriften. Sie besitzt keine Urheberrechte an den Zeitschriften und ist nicht verantwortlich für deren Inhalte. Die Rechte liegen in der Regel bei den Herausgebern beziehungsweise den externen Rechteinhabern. [Siehe Rechtliche Hinweise.](#)

Conditions d'utilisation

L'ETH Library est le fournisseur des revues numérisées. Elle ne détient aucun droit d'auteur sur les revues et n'est pas responsable de leur contenu. En règle générale, les droits sont détenus par les éditeurs ou les détenteurs de droits externes. [Voir Informations légales.](#)

Terms of use

The ETH Library is the provider of the digitised journals. It does not own any copyrights to the journals and is not responsible for their content. The rights usually lie with the publishers or the external rights holders. [See Legal notice.](#)

Download PDF: 15.03.2025

ETH-Bibliothek Zürich, E-Periodica, <https://www.e-periodica.ch>

Epitaxy of hedenbergite whiskers on babingtonite in Alpine fissures at Arvigo, Val Calanca, Grisons, Switzerland

by Thomas Armbruster¹, Hans Anton Stalder², Edwin Gnos³, Beda Hofmann⁴ and Marco Herwegh⁵

Abstract

In a small sample from a low-temperature hydrothermal fissure at Arvigo, Val Calanca, epitaxial whiskers of hedenbergite $\text{Ca}(\text{Fe}^{2+}, \text{Mg}, \text{Mn})[\text{Si}_2\text{O}_6]$ on the pyroxenoid babingtonite $\text{Ca}_2(\text{Fe}^{2+}_{0.46}\text{Mg}_{0.28}\text{Mn}^{2+}_{0.26})(\text{Fe}^{3+}_{0.97}\text{Al}_{0.03})[\text{Si}_5\text{O}_{14}(\text{OH})]$ (space group $P\bar{1}$, $a = 7.480(1)$, $b = 12.159(1)$, $c = 6.678(2)$ Å, $\alpha = 86.10(2)$, $\beta = 93.92(1)$, $\gamma = 112.08(1)^\circ$, $V = 560.9(2)$ Å³) were analyzed by single-crystal X-ray methods, scanning electron microscopy, and electron microprobe analyses. The Zweier-einfachketten of hedenbergite (pyroxene) were found to be coherent with the Fünfer-einfachketten of babingtonite. The epitaxial babingtonite-pyroxene intergrowth is associated with heulandite, chlorite, and minor fluorite. It is assumed that hedenbergite grew out of babingtonite when the oxygen fugacity decreased at a late stage of the fissure development. Babingtonite from Alpine fissures exhibits pronounced substitution of Mg and Mn^{2+} for Fe^{2+} .

Keywords: babingtonite, hedenbergite, Alpine fissures, epitaxy, Arvigo, Grisons.

Introduction

Babingtonite, $\text{Ca}_2\text{Fe}^{2+}\text{Fe}^{3+}[\text{Si}_5\text{O}_{14}(\text{OH})]$, a pyroxenoid group mineral, is characteristic of zeolitic veins and cavities in basic igneous rocks and granites (e.g., BURT, 1971; FRANZINI et al. 1978; BIRCH, 1983; WISE and MÖLLER, 1990) but has also been reported from skarn deposits (e.g., GOLE, 1981; BURNS and DYAR, 1991). Other occurrences are in pegmatites (JANECEK and SACHANBINSKI, 1992; ORLANDI et al., 1998) and in calcareous volcanic detritus (DUGGAN, 1986). BIRCH (1983) estimated for babingtonite in zeolitic veins at Harcourt, Victoria, Australia, crystallization conditions of the order of 0.5 kbar between 100 and 150 °C. Similar conditions of 150–200 °C and ca. 0.5 kbar were reported for babingtonite from cavities of the Deccan basalts in India (WISE and MÖLLER, 1990). Other Ca–Fe–silicates commonly associated with babingtonite are ilvaite $\text{CaFe}^{2+}_2\text{Fe}^{3+}\text{O}(\text{OH})[\text{Si}_2\text{O}_7]$, hedenbergite

$\text{CaFe}[\text{Si}_2\text{O}_6]$, julgoldite $\text{Ca}_2\text{Fe}^{2+}\text{Fe}^{3+}_2(\text{OH})_2[\text{SiO}_4][\text{Si}_2\text{O}_7]\cdot\text{H}_2\text{O}$ (the ferric iron analogue of pumpellyite), and andradite $\text{Ca}_3\text{Fe}^{3+}_2[\text{SiO}_4]_3$ (BURT, 1971).

The chemical composition of babingtonite is remarkably consistent with the idealized formula with mainly Mn^{2+} and Mg substituting for Fe^{2+} . Manganbabingtonite, $\text{Ca}_2(\text{Mn}^{2+}, \text{Fe}^{2+})\text{Fe}^{3+}[\text{Si}_5\text{O}_{14}(\text{OH})]$, has also been reported as an independent species from skarn deposits (VINOGRADOVA et al., 1966; BURT and LONDON, 1978). Recently, the scandium analogue, scandiobabingtonite, $\text{Ca}_2(\text{Fe}^{2+}, \text{Mn}^{2+})\text{Sc}[\text{Si}_5\text{O}_{14}(\text{OH})]$, has been defined from the Baveno pegmatite, Piedmont, Italy (ORLANDI et al., 1998).

Babingtonite is triclinic (space group $P\bar{1}$) and has a Fünfer-einfachkette of $[\text{Si}_5\text{O}_{14}(\text{OH})]$ composition (ARAKI and ZOLTAI, 1972; KOSOI, 1976). Hydrogen occurs as a silanol group (Si–OH), hydrogen bonded to an adjacent tetrahedron of the same chain unit (TAGAI et al., 1990). CZANK (1981), performing a high resolution electron

¹ Laboratorium für chemische und mineralogische Kristallographie, Universität Bern, Freiestr. 3, CH-3012 Bern, Switzerland. <thomas.armbruster@krist.unibe.ch>

² Pelikanweg 40, CH-3074 Muri, Switzerland.

³ Mineralogisch-Petrographisches Institut, Universität Bern, Baltzerstr. 1, CH-3012 Bern, Switzerland.

⁴ Naturhistorisches Museum, Bernastr. 15, CH-3005 Bern, Switzerland.

⁵ Geologisches Institut, Universität Bern, Baltzerstr. 1, CH-3012 Bern, Switzerland.

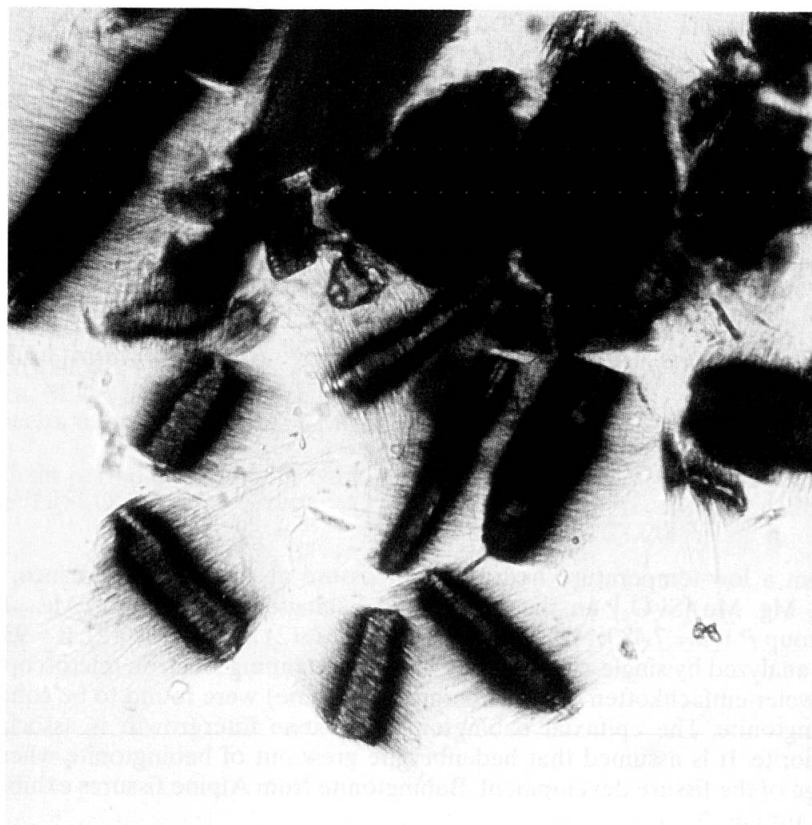


Fig. 1 Microscopical photograph (planar polarized light) of babingtonite crystals with epitaxial hedenbergite whiskers; base of image is 1.6 mm.

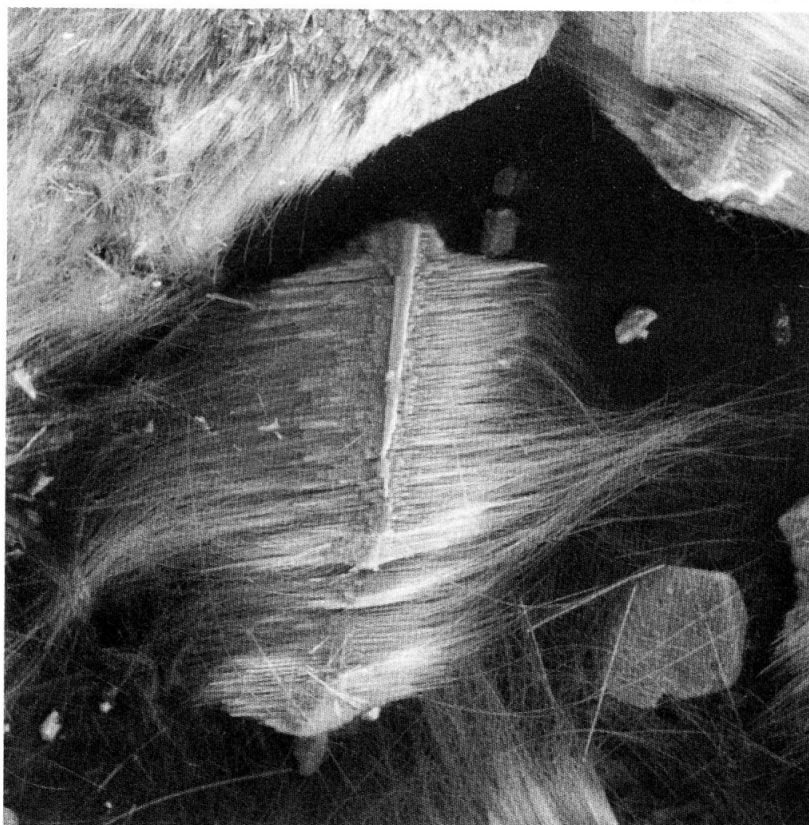


Fig. 2 Scanning electron microscopic picture of composite babingtonite-hedenberite crystals. The base of the picture is 0.174 mm. Babingtonite forms the central back bone out of which epitaxial whiskers of hedenbergite grew.

microscopic study, recognized planar chain periodicity faults giving rise to domains with chain translations of 3, 7, 9 and 11 tetrahedra.

The first and only occurrence of babingtonite in Switzerland was reported by GRAESER and STALDER (1976) from Alpine fissures in a gneiss of the quarry at Arvigo in Val Calanca, Grisons. At this locality black babingtonite crystals are associated with epidote, titanite, prehnite, adularia, chlorite, and calcite.

Sample description

The so called 'Calancagrani' (mainly used as building stone) mined at Arvigo (Grisons) is actually a banded biotite gneiss intercalated with more massy, light coloured two mica gneiss and less frequently with calcsilicate lenses. Tectonically the rocks belong to the upper Simano nappe. Among collectors the Arvigo quarries became famous for the large number of Alpine fissure minerals. Most of the fissure minerals belong to the so called 'Fundortgruppe 10g' (WAGNER and STALDER, 2000a,b) characterized by the assemblage epidote, prehnite, and various zeolites. In general, epidote is overgrown by prehnite and zeolites, indicating that epidote is one of the primary minerals within this late fissure mineral assemblage. A very rare mineral in the same 'Fundortgruppe 10g' at Arvigo is vanadinite (CUCHET et al., 1995). Fluid inclusion measurements on fissure quartz (WAGNER and STALDER, 2000a,b) yielded two generations, CO₂ rich (35–70 vol%) inclusions in the central parts of quartz which homogenize above 310 °C and rather salt-poor water inclusions (gas bubble and liquid H₂O) in the rims of the quartz crystals. These latter inclusions homogenize between 160 °C and 180 °C. Solid inclusions in the quartz rims are fibrous actinolite, epidote, chlorite, and occasionally calcite. These minerals are all characteristic of the epidote–prehnite–zeolite fissure group. Frequently, the quartz rim and core are separated by layers of fibrous actinolite. These observations suggest that 160–180 °C is the minimum temperature (neglecting a pressure correction) for the formation of the epidote–prehnite–zeolite assemblage.

The sample (NMBE 34974) studied in this paper is ca. 4 × 2 × 2 cm³ and consists of few intergrown heulandite crystals. Heulandite appears greenish due to inclusions of chlorite. The crystal surfaces and interstices are covered with chlorite, and few small octahedral fluorite crystals. Striking are abundant composite aggregates, ca. 0.15 mm in maximum dimension, composed of a green central crystal with a dense, white felt attached to it.

The asbestos like fibers of the felt are grown parallel to each other, nearly perpendicular to the elongation of the central crystal. Thus, when viewed with the binocular the composites appear as tiny 'sandwiches'. When the composites are immersed in oil and viewed with a polarizing microscope the dominant green crystals in the center can be well distinguished from the attached whiskers (Fig. 1). In contrast, only a narrow ridge of the central crystal can be seen and the thin epitaxial whiskers dominate the appearance when imaging the morphology of the composites with a scanning electron microscope (Fig. 2).

Energy dispersive analyses (EDA) performed with a scanning electron microscope gave the approximate compositions Ca₂(Fe_{1.2}Mn_{0.5}Mg_{0.2}Al_{0.1})[Si₅O₁₄(OH)] and Ca₂(Fe_{0.8}Mn_{0.5}Mg_{0.6}Al_{0.1})[Si₅O₁₄(OH)] for the central crystal (after normalization for babingtonite stoichiometry, see below). The thin fibers, epitaxially attached to babingtonite, had the approximate composition Ca(Fe_{0.5}Mg_{0.3}Mn_{0.2})[Si₂O₆] (after normalization to pyroxene stoichiometry, see below).

Experimental

Using a binocular, composite crystals were shaved with a scalpel to remove the attached whiskers. One separated crystal, 0.10 × 0.10 × 0.05 mm³ in size, appeared transparent, bottle green and was only covered with few bristles. This specimen was used for further investigation with an Enraf Nonius CAD4 and a Siemens SMART system equipped with a CCD area detector. Both diffractometers were operated with graphite monochromatized MoK α X-radiation. Using the CAD4 precise cell dimensions were determined from 25 reflection positions with $\theta > 15^\circ$.

In an additional experiment several composite crystals were glued on the tip of a fine glass fiber (0.05 mm in diameter) and a rotation diffraction pattern was recorded with the CCD camera of the SMART system. This picture revealed sharp spots from the central babingtonite crystals (which were ignored) and Debye-Scherrer rings of the fine whiskers. SMART software enabled direct determination of the *d*-spacings of the Debye-Scherrer rings. Subsequently, the ten strongest powder diffractions were submitted to a powder pattern identification program (MPDS by HUMMEL, 1990).

Babingtonites were analyzed by electron microprobe (Cameca SX-50) using beam conditions of 15 kV and 20 nA, an enlarged spot size of ca. 10 μ m, and wavelength-dispersive mode. The following natural and synthetic standards and

Tab. 1 Electron microprobe analyses (wt%) of babingtonites (average of ten point analyses) from Arvigo (Grisons) and Westfield (Mass.). Formula calculation was normalized to nine cations.

	Arvigo ¹ average	range	Arvigo ² average	range	Westfield average	range
SiO ₂	53.35	52.46–54.05	53.63	53.15–53.88	53.13	52.85–53.48
Al ₂ O ₃	0.74	0.38–1.09	0.31	0.20–0.54	0.49	0.35–0.72
FeO ^a	18.97	17.93–19.84	18.04	17.87–19.25	21.49	20.88–22.42
MnO	2.58	2.22–3.01	3.35	2.07–3.72	0.77	0.39–1.11
MgO	1.58	1.16–2.32	2.04	1.84–2.27	1.24	0.98–1.43
CaO	19.81	19.66–20.05	19.85	19.73–20.11	19.77	19.64–19.88
Na ₂ O	0.04	0.02–0.09	0.04	0.02–0.07	0.03	0.01–0.05
Σ ^b	97.07		97.26		96.92	
Si	5.01		5.02		5.01	
Al	0.08		0.03		0.05	
Fe	1.49		1.41		1.70	
Mn	0.21		0.26		0.06	
Mg	0.22		0.28		0.18	
Ca	1.99		1.99		2.00	
Na	0.01		0.01		0.00	

¹ isolated single crystals (NMBE 34973) as described by GRAESER and STALDER (1976).

² composite crystals with epitaxial hedenbergite (NMBE 34974)

^a all Fe was calculated as FeO.

^b H₂O contributed by the OH group was not determined explaining the low sums.

spectrometer crystals were used (generally K α lines): orthoclase, K (PET) and Si (TAP); anorthite, Al (TAP) and Ca (PET); spinel, Mg (TAP); almandine, Fe (LIF); albite, Na (TAP); tephroite, Mn (LIF), and ilmenite, Ti (PET). Data were collected for 20 seconds on peak and background. For comparison, analyses (Tab. 1) were also performed for babingtonite from Arvigo without epitaxial hedenbergite, previously described by GRAESER and STALDER (1976). This second Arvigo sample consists mainly of adularia on which epidote and babingtonite crystallized. All minerals are encrusted by chlorite. The other reference sample is a babingtonite from a skarn at Westfield, Mass., USA.

Results

Single-crystal X-ray data for the central crystal yielded a triclinic cell with $a = 7.480(1)$, $b = 11.637(1)$, $c = 6.678(2)$ Å, $\alpha = 91.55(2)$, $\beta = 93.92(2)$, $\gamma = 104.48(1)^\circ$, $V = 560.9(2)$ Å³. These crystallographic data combined with the approximate chemical composition led to the straight-forward identification as babingtonite. The above reduced cell was subsequently transformed (matrix: [1 0 0; 1 1 0; 0 0 -1]) to a non-standard cell with $a = 7.480(1)$, $b = 12.159(1)$, $c = 6.678(2)$ Å, $\alpha = 86.10(2)$, $\beta = 93.92(1)$, $\gamma = 112.08(1)^\circ$, $V = 560.9(2)$ Å³. The latter setting has the advantage that the silicate Fünfer-einfachketten run parallel to the b -axis.

The X-ray powder identification program listed for the whiskers seven clinopyroxenes (hedenbergite, diopside, johannsenite, and additional solid solutions). The chemical composition normalized to pyroxene stoichiometry identified the mineral as a hedenbergite-rich member of the hedenbergite–diopside–johannsenite solid solution series. Such a crystal has the approximate cell dimensions (space group $C2/c$) $a = 9.80$, $b = 8.99$, $c = 5.24$ Å, $\beta = 105.3^\circ$.

Due to the thin nature of the hedenbergite whiskers, the epitaxial relation between babingtonite and the pyroxene could only qualitatively be evaluated. In Alpine fissures diopside and hedenbergite are commonly elongated parallel to the c -axis, the direction of the silicate Zweier-einfachkette (e.g., STALDER et al. 1998). Thus we assumed that the hedenbergite whiskers are also extended parallel to the c -axis. The epitaxial relation was studied with a microscope attached to the X-ray diffractometer such that indexed crystal faces could be viewed. The pyroxene whiskers emerge out of the babingtonite (010) face (in non-standard setting) and are aligned approximately parallel to [010]_{bab}. Babingtonite crystals are elongated parallel to [001]. Thus the pyroxene whiskers form a 'curtain' parallel to the b – c plane of babingtonite. In other words, the Fünfer-einfachketten in babingtonite are probably coherent with the Zweier-einfachketten in the pyroxene. These observed orientation relations are in line with the periodicity faults in babingtonite de-

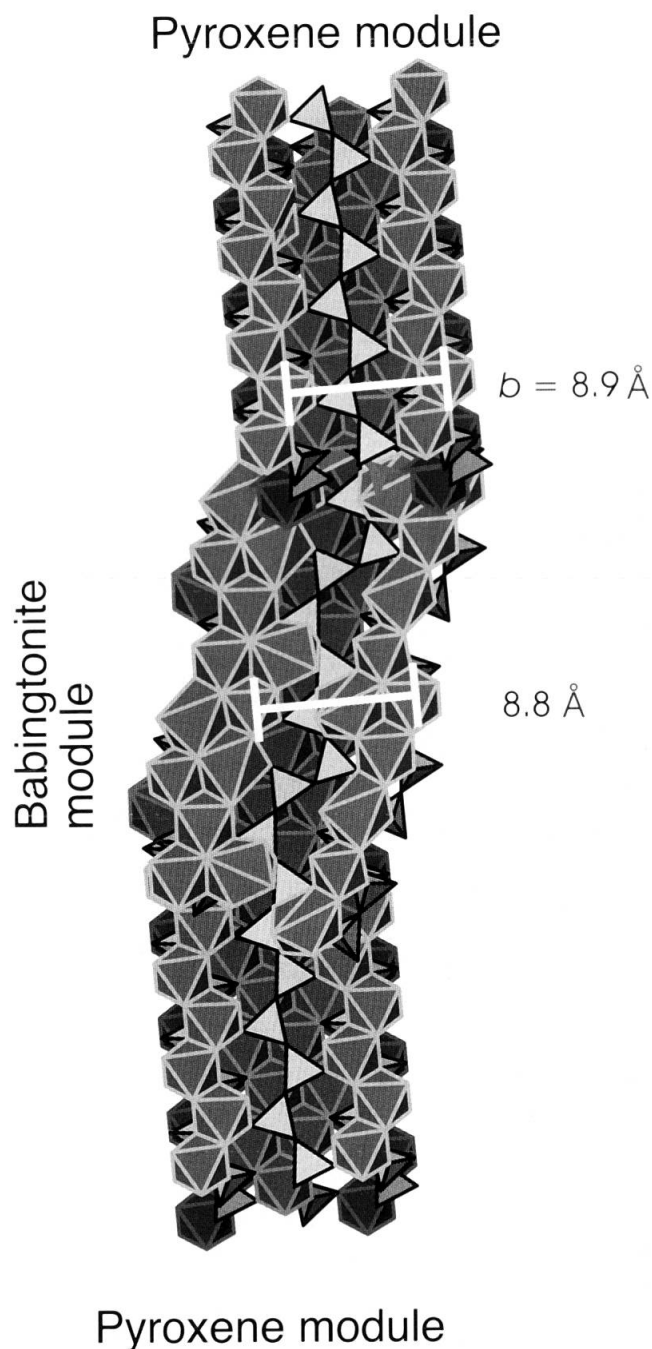


Fig. 3 Polyhedral drawing explaining the epitaxial relation between the structures of babingtonite and hedenbergite as a coherent intergrowth of a central babingtonite module with two attached pyroxene modules. The silicate chain of babingtonite has a periodicity of five tetrahedra whereas pyroxene has a periodicity of two tetrahedra. The b -axis of pyroxene (ca. 8.9 \AA) is parallel to a 8.8 \AA vector in babingtonite that has no true translational component because it connects two polyhedra which are not symmetrically equivalent.

scribed by CZANK (1981) using high resolution electron microscopy. In figure 3 we attached to both sites of a babingtonite module (representing the central crystal) two hedenbergite modules,

thus a continuous transition of a Fünfer-einfachkette to a Zweier-einfachkette was obtained. In addition, a coherent orientation of the other coordination polyhedra in both structures was attempted (Fig. 3). In hedenbergite a (001) octahedral-tetrahedral-octahedral slab is ca. 4.7 \AA thick ($a/2 \cos(\beta-90^\circ)$). A corresponding slab in babingtonite occurs along [101], non-standard setting, and is ca. 4.8 \AA thick. The b -axis (8.9 \AA) in hedenbergite corresponds to a 8.8 \AA vector in babingtonite (Fig. 3) that has no true translational component because it connects two polyhedra which are not symmetrically equivalent.

Discussion

Babingtonite has been reported associated with the calcium zeolites laumontite (WISE and MOLLER, 1990) and stellerite (BIRCH, 1983; BIRCH interpreted this zeolite as stilbite but its low Na content is characteristic of stellerite). At Arvigo babingtonite is associated with heulandite and sometimes the composite babingtonite-hedenbergite assemblages are even overgrown by heulandite suggesting similar stability relations. The temperature estimates for the laumontite-babingtonite (ca. $200 \text{ }^\circ\text{C}$) and stellerite-babingtonite assemblages ($100\text{--}150 \text{ }^\circ\text{C}$) are based on field evidence and calcite fluid inclusion measurements (BIRCH, 1983; WISE and MOLLER, 1990) and conform with the stability relations of zeolites found in the geothermal areas in Iceland (KRISTMANNSDOTTIR and TOMASSON, 1978). Heulandite at Iceland was found below ca. $< 200 \text{ }^\circ\text{C}$ as stellerite, but may also extend to temperatures below $70 \text{ }^\circ\text{C}$. The upper temperature limit of approximately $200 \text{ }^\circ\text{C}$ for crystallization of heulandite and babingtonite at Arvigo is also confirmed by the fluid inclusion measurements in the rims of quartz crystals (WAGNER and STALDER, 2000a,b).

The epitaxial growth of hedenbergite on babingtonite can be explained by variation of f_{O_2} within the fissures. At high oxygen fugacity babingtonite is formed; with decreasing oxygen fugacity hedenbergite nucleates on pre-existing babingtonite, leading to the observed epitaxial relation. We are not aware of other occurrences of hedenbergite whiskers. Thus this acicular habit may be specific of epitaxial growth.

The chemical composition (Tab. 1) of the low-temperature fissure babingtonites from Arvigo deviates strongly from the close to end-member composition usually found for babingtonites from skarn deposits (e.g., BURNS and DYAR, 1991). Babingtonites associated with zeolites at Arvigo are enriched in Mg and Mn^{2+} replacing Fe^{2+} .

Notice that semi-quantitative EDA analyses with the scanning electron-microscope even suggested that the composite babingtonite should be considered manganbabingtonite or 'magnesiumbabingtonite'. It is not clear though whether this is an artifact of the EDA analyses or whether the analyzed (latest stage) surface of these specific crystals was more Mn- and Mg-rich. Enrichment of Mg was also described by WISE and MOLLER (1990) for babingtonites occurring together with laumontite in the Deccan Trap basalts in India and by FRANZINI et al. (1978) for a babingtonite-quartz-prehnite assemblage.

Acknowledgement

The constructive reviews of S. Graeser (Basel) and G. Amthauer (Salzburg) are highly acknowledged.

References

- ARAKI, T. and ZOLTAI, T. (1972): Crystal structure of babingtonite. *Z. Kristallogr.*, 135, 355–373.
- BIRCH, W.D. (1983): Babingtonite, fluorapophyllite and sphene from Harcourt, Victoria, Australia. *Mineral. Mag.*, 47, 377–380.
- BURNS, R.G. and DYAR, M.D. (1991): Crystal chemistry and Mössbauer spectra of babingtonite. *Am. Mineral.*, 76, 892–899.
- BURT, D.M. (1971): Multisystems analysis of the relative stabilities of babingtonite and ilvaite. *Carnegie Inst., Annu. Rep. Geophys. Lab.*, 70, 189–197.
- BURT, D.M. and LONDON, D. (1978): Manganbabingtonite and ilvaite from a hedenbergite-johannsenite skarn, Aravaipa, Arizona. *Geol. Soc. Am., Abs. with Prog.*, 10/3, 98.
- CUCHET, S., GRAESER, S., MEISSER, N., RÖHRNBAUER, H. and WEISS, S. (1995): Vanadinit – ein ungewöhnliches Kluftmineral aus den Alpen. *Lapis*, 20, IX, 37–41.
- CZANK, M. (1981): Chain periodicity faults in babingtonite, $\text{Ca}_2\text{Fe}^{2+}\text{Fe}^{3+}\text{H}[\text{Si}_5\text{O}_{15}]$. *Acta Cryst.*, A37, 617–620.
- DUGGAN, M.B. (1986): Babingtonite and Fe-rich Ca–Al silicates from western Southland, New Zealand. *Mineral. Mag.*, 50, 657–665.
- FRANZINI, M., LEONI, L., MELLINI, M. and ORLANDI, P. (1978): The babingtonite of Figliini (Prato), Italy. *Rend. Soc. Ital. Mineral. Petrol.*, 34, 45–50.
- GOLE, M.J. (1981): Ca–Fe–Si skarns containing babingtonite: first known occurrence in Australia. *Can. Mineral.*, 19, 269–277.
- GRAESER, S. and STALDER, H.A. (1976): Mineral-Neufunde aus der Schweiz und angrenzenden Gebieten II. *Schweizer Strahler*, 4, 158–171.
- HUMMEL, W. (1990): MPDS, mineral powder diffraction search program. *Laboratorium für chemische und mineralogische Kristallographie, Universität Bern.*
- JANECZEK, J. and SACHANBINSKI, M. (1992): Babingtonite, Y–Al-rich titanite, and zoned epidote from the Strzegom pegmatites, Poland. *Eur. J. Mineral.*, 4, 307–319.
- KOSOI, A.L. (1976): The structure of babingtonite. *Sov. Phys. Crystallogr.*, 20, 446–451.
- KRISTMANNSDOTTIR, H. and TOMASSON, J. (1978): Zeolite zones in geothermal areas in Iceland. In: SAND, L.B. and MUMPTON, F.A. (eds): *Natural Zeolites: Occurrence, Properties and Use*. Pergamon Press, 277–284.
- ORLANDI, P., PASERO, M. and VEZZALINI, G. (1998): Scandiobabingtonite, a new mineral from the Baveno pegmatite, Piedmont, Italy. *Am. Mineral.*, 83, 1330–1334.
- STALDER, H.A., WAGNER, A., GRAESER, S. and STUKER, P. (1998): *Mineralienlexikon der Schweiz*. Wepf Verlag, Basel, 379 pp.
- TAGAI, T., JOSWIG, W. and FUESS, H. (1990): Neutron diffraction study of babingtonite at 80 K. *Mineral. J.*, 15, 8–18.
- VINOGRADOVA, R.A., SYCHKOVA, V.A. and KABALOV, YU.K. (1966): Manganiferous babingtonite from the Rudny Kaskad deposit, Eastern Sayan (in Russian). *Dokl. Akad. Nauk USSR*, 169, 434–437.
- WAGNER, A. and STALDER, H.A. (2000a): Arvigo – eine der bekanntesten Mineralfundstellen der Schweiz, Teil 1. *Schweizer Strahler*, 12, 41–60.
- WAGNER, A. and STALDER, H.A. (2000b): Arvigo – eine der bekanntesten Mineralfundstellen der Schweiz, Teil 2. *Schweizer Strahler*, 12, 118–133.
- WISE, W.S. and MOLLER, W.P. (1990): Occurrence of Ca–Fe silicate minerals with zeolites in basalt cavities at Bombay, India. *Eur. J. Mineral.*, 2, 875–883.

Manuscript received April 28, 2000; revision accepted August 22, 2000.